Influence of Valley Splitting on Spin Relaxation Time in a Strained Thin Silicon Film

Joydeep Ghosh, Viktor Sverdlov, and Siegfried Selberherr
Institute for Microelectronics, TU Wien, Gußhausstraße 27–29/E360, A–1040 Wien, Austria
Email: {ghosh|sverdlov|selberherr}@iue.tuwien.ac.at

***Abstract*—The electron spin properties are promising for future spin-driven devices. In contrast to charge, spin is not a conserved quantity, and having sufficiently long spin lifetime is critical for applications. Silicon, the major material of microelectronics, also appears to be a perfect material for spintronic applications. The peculiarities of the subband structure and details of the spin propagation in ultra-thin silicon films in the presence of strain are investigated. The application of an uniaxial stress can lift the degeneracy between the remaining two valleys in a (001) silicon film. The [001] equivalent valley coupling through the Γ-point, which results in a subband splitting in a confined relaxed electron structure, is properly included. Its impact on the shear strain inflicted equivalent subband splitting is evaluated, and thereby the dependence of spin lifetime on the valley splitting is predicted. In all possible conditions, the spin lifetime is observed to be boosted by several orders of magnitude.**

I. Introduction

Recent advances in semiconductor device shrinking and development of multi-core processor architectures have continuously boosted the performance of modern computers. However, increasing technological challenges and soaring costs are gradually guiding MOSFET scaling to an end [1], which is driving the search for alternative technologies. MOSFET operation in modern days is principally based on the charge degree of freedom of an electron. Another intrinsic electron property, the electron spin, attracts at present much attention as a possible candidate for complementing or even replacing the charge degree of freedom in future electronic devices. Using electron spin may help to reduce power consumption and increase the computational speed of modern electronic circuits [2]. Because of the paramount importance of SOI and FinFET 3D technology for technology nodes from the 22nm to the 14nm nodes and even beyond, spin lifetime in such structures is a very relevant issue under inspection.

Silicon is a popular material for spin-driven applications, particularly due to its high spin lifetime [3]. The lower estimate for the spin lifetime at room temperature obtained within the three-terminal injection scheme is of the order 0.1-10ns [3]. The first demonstration of coherent spin transport through an undoped 350μm thick silicon wafer [4] has triggered a systematic study of spin transport properties in silicon. The possibility of injecting spin at room temperature [5] makes the fabrication of spin-based switching devices quite plausible in the near future. On the contrary, a large experimentally observed spin relaxation in electrically-gated silicon structures could become an obstacle in realizing spin-driven devices [6]. Hence, a deeper understanding of the fundamental spin relaxation mechanism in silicon MOSFETs is needed.

Shear strain has been traditionally used to boost electron mobility. We investigate the surface roughness (SR), and electron-phonon (Ph) limited spin relaxation time behavior in a (001) oriented thin silicon film subjected to [110] uniaxial tensile stress known to produce a shear strain (ε_{xy}). The longitudinal (LA) and the transversal (TA) acoustic phonons are under consideration [7], as the contribution of optical phonons can be safely ignored for a film thickness of less than 3nm. In order to evaluate the subband wave functions and spin flip matrix elements we use the $\mathbf{k}\cdot\mathbf{p}$ Hamiltonian [8] [9] with spin degree of freedom [10], written at the vicinity of the X-point for the two relevant [001] valleys along the OZ-axis in the Brillouin zone. Valley splitting in a silicon quantum well at zero strain as a function of the quantum well width has been known for a long time [11]. The values of the valley splitting [12] obtained from a 30-band $\mathbf{k}\cdot\mathbf{p}$ model [13] and sp^{3}d^{5}s* spin-orbit coupled tight-binding model [14] can be considered. This impacts the valley splitting under shear strain, the spin relaxation matrix elements, and finally the spin-flip mechanisms. The obtained results are compared.

II. Model

A. Valley Splitting in Relaxed Silicon

The valley splitting in unstrained films can be expressed following [12] as:

$$\triangle E_C = \frac{2\pi^2\Lambda_\Gamma}{(k_{0\Gamma}t)^3}\cdot|\sin(k_{0\Gamma}t)|\,, \tag{1}$$

Parameter	Value
Silicon lattice constant	a=0.5431nm
Spin-orbit term	$\triangle_{SO}$=1.27meVnm [7]
Shear deformation potential	D=14eV
Acoustic deformation potential	Ξ=12eV
Yafet type factor due to the spin-orbit interaction	D_{SO}=15meV/k_0 [15]
Electron rest mass in silicon	m_e
Transversal effective mass	$m_t = 0.19\,m_e$
Longitudinal effective mass	$m_l = 0.91\,m_e$
Valley minimum position from X-point	$k_0 = 0.15\cdot\frac{2\pi}{a}$
Splitting at Γ-point	Λ_Γ in eV
$k_{0\Gamma}$	$k_{0\Gamma} = 0.85\cdot\frac{2\pi}{a}$

TABLE I: Simulation parameter list

978-0-692-51523-5/15/$31.00 © 2015 IEEE

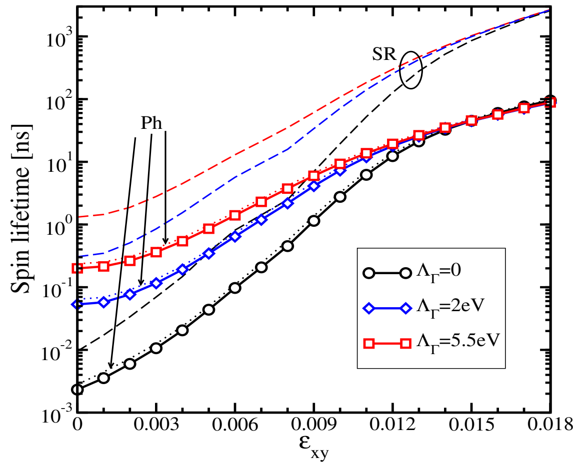

Fig. 1: Variation of SR- and Ph-mediated spin lifetime with ε_{xy}, when different possible values for Λ_Γ are considered. t=2.7nm, N_S=10^{12}cm^{-2}, T=300K.

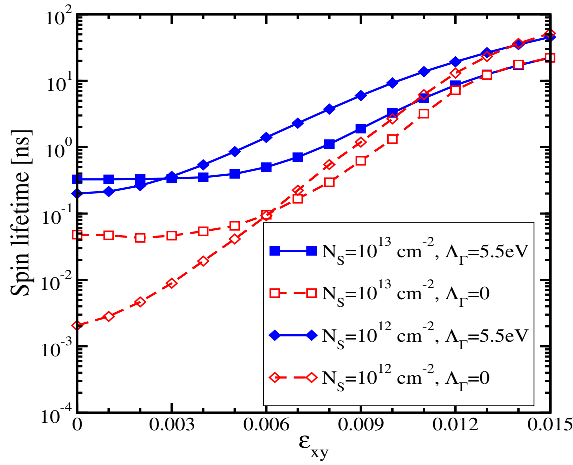

Fig. 2: Variation of the spin lifetime with ε_{xy} with the electron concentration as parameter. t=2.7nm, T=300K.

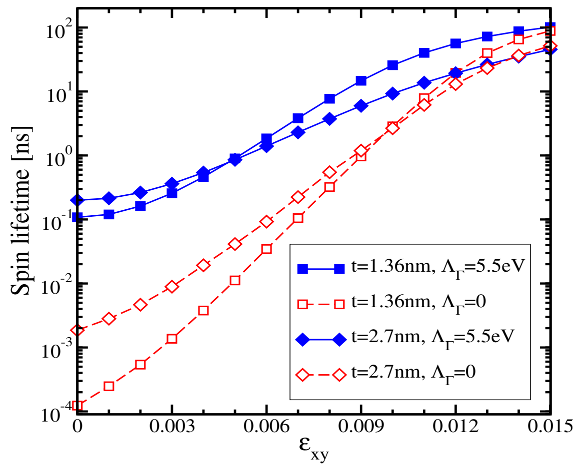

Fig. 3: Variation of the spin lifetime with ε_{xy} with the sample thickness as parameter. N_S=10^{12}cm^{-2}, T=300K.

where t is the film thickness, and the other parameters as listed in Table I. Λ_Γ is a parameter defining the strength of the valley-orbit interaction with its value ranging between 2eV (30-band $\mathbf{k}\cdot\mathbf{p}$ model) and 5.5eV (tight-binding model), depending on the approach used to evaluate the band structure. Both methods reproduce the features of the conduction and valence band equally well, but require additional experimental verification at higher energies, where the discrepancy appears.

B. *The* $\mathbf{k}\cdot\mathbf{p}$ *Hamiltonian with Spin Degree of Freedom*

The effective two-band $\mathbf{k}\cdot\mathbf{p}$ Hamiltonian, including the spin degree of freedom and shear strain, describes the electron states in the conduction band of the two relevant [001] valleys in the vicinity of the X-point along the OZ-axis in the Brillouin zone.

The Hamiltonian can be expressed following [10] as:

$$H = \begin{bmatrix} H_1 & H_3 \\ H_3 & H_2 \end{bmatrix}, \tag{2}$$

with

$$H_{j=1,2} = \left[\frac{\hbar^2 k_z^2}{2m_l} + \frac{\hbar^2\left(k_x^2+k_y^2\right)}{2m_t} + (-1)^j\delta + U(z)\right] I \tag{3}$$

$$H_3 = \begin{bmatrix} \dfrac{\hbar^2 k_0 k_z}{m_l} & 0 \\ 0 & \dfrac{\hbar^2 k_0 k_z}{m_l} \end{bmatrix}, \tag{4}$$

where (k_x, k_y, k_z) represents the projections of the $\vec{k}$ vector on the coordinate axes, $U(z)$ is the confinement potential, $M^{-1} = m_t^{-1} - m_e^{-1}$, and the other parameters are defined in Table I. The value for δ is

$$\delta = \sqrt{\left(D\varepsilon_{xy} - \frac{\hbar^2 k_x k_y}{M}\right)^2 + \triangle_{SO}^2(k_x^2+k_y^2) + \left(\frac{k_0}{k_{0\Gamma}}\right)^6 {\Lambda_\Gamma}^2}. \tag{5}$$

The energy dispersion relation can thus be written as

$$E(k_z) = \frac{\hbar^2 k_z^2}{2m_l} + \frac{\hbar^2(k_x^2+k_y^2)}{2m_t} \pm \sqrt{\left(\frac{\hbar^2 k_z k_0}{m_l}\right)^2 + \delta^2}. \tag{6}$$

The individual spin relaxation time components are calculated by the corresponding thermal averaging of the respective subbands in-plane momentum dependent scattering rates [7] [15] [16] [17]. The total spin lifetime (τ_S) is evaluated by the Matthiessen rule [18].

III. Results

A. *Spin Lifetime with Strain*

We analyze the variations of the SR- and Ph-mediated spin relaxation components of τ_S with ε_{xy}, with and without including the parameter Λ_Γ into the computation (Figure 1). One can observe a giant increment of the components, when Λ_Γ is not included. The increase is less pronounced, when the value of Λ_Γ increases. However, even when Λ_Γ is taken to be 5.5eV, the value of τ_S increases by two orders of magnitude.

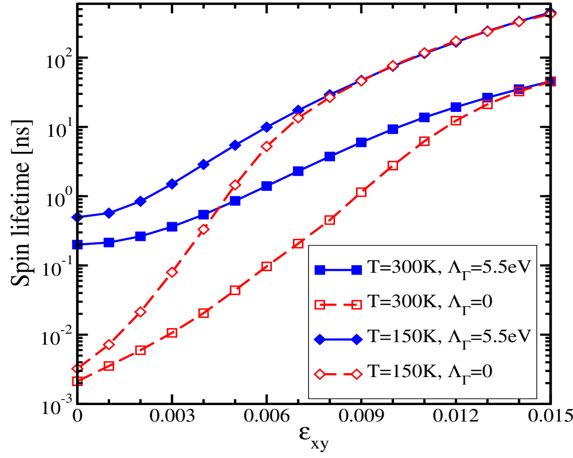

Fig. 4: Variation of the spin lifetime with ε_{xy} with the temperature as parameter. N_S=10^{12}cm^{-2}, t=2.7nm.

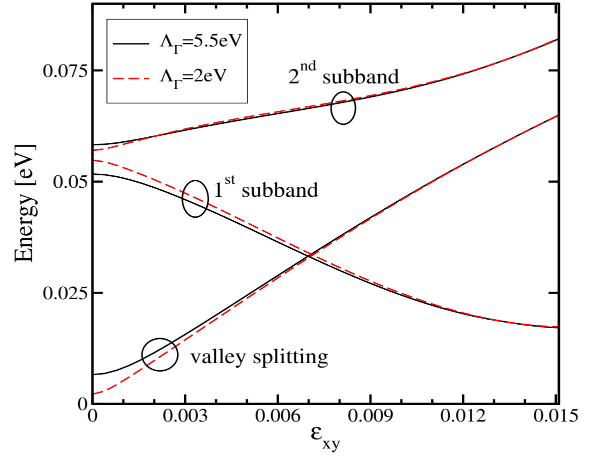

Fig. 5: The minimum energies of two lowest unprimed subbands with ε_{xy} at two distinct Λ_Γ values. N_S=10^{12}cm^{-2}, t=2.7nm, T=300K.

It is further noted that for a film thickness of t=2.7nm, the acoustic phonon-induced spin-flip mechanism is dominating in all three distinct cases.

Now we analyze the variation of τ_S with ε_{xy}, when the electron concentration (N_S) is used as a parameter, c.f. Figure 2. The spin relaxation becomes less severe for higher carrier concentrations for all considered mechanisms. This happens due to the lifting of the Fermi level with increasing concentration. Figure 3 shows the increase in τ_S with ε_{xy} for different values of t. Figure 4 describes how τ_S is sensitive to the operating temperature (T). The figure confirms that at higher temperature where the phonon scattering rate is significantly increased, the value of τ_S is shorter as compared to its value at lower temperature, at each strain point. From these results we can conclude that τ_S is distinguishably sensitive on the operating parameters like t, N_S, and T. In all cases, the increase of τ_S becomes less pronounced when Λ_Γ is high. It is also noted that at high ε_{xy}, the values of τ_S become the same with respect to the values of Λ_Γ.

B. Inter- and Intravalley Transition

In order to elucidate the spin relaxation mechanism, we consider the spin-flip caused by the intra- and inter- valley transitions. Figure 5 shows the minimum energy levels (when k_x=k_y=0) of the two lowest unprimed subbands primarily responsible [19] [20] for the spin relaxation, for several Λ_Γ. The unprimed subbands are degenerate at zero strain without the Λ_Γ term. The Λ_Γ term lifts the degeneracy even at zero strain. The figure also shows how an increasing ε_{xy} inflicts the subband splitting between the unprimed valley pair. This splitting pushes out the regions of large mixing between the spin-up and spin-down states to higher kinetic energies outside of the occupied states. With increasing ε_{xy}, the influence of Λ_Γ vanishes as is obvious from (6). Nevertheless, this lifting of the degeneracy is the crucial factor for the spin lifetime enhancement. We point out that the degeneracy between equivalent valleys was a longstanding problem in silicon spintronics.

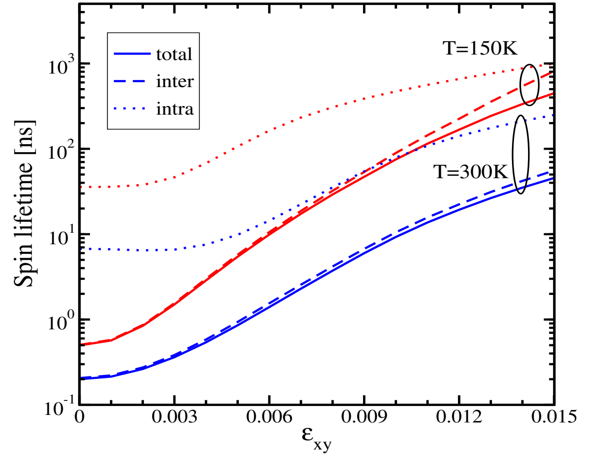

Fig. 6: Spin relaxation time with the respective components. N_S=10^{12}cm^{-2}, t=2.7nm.

Figure 6 depicts the inter- and intravalley scattering components of τ_S at two distinct values of T. It is observed that the major contribution to the spin relaxation comes from the intervalley transition process, which is significantly reduced at high strain, in accordance with Figure 5. At high valley splitting, the spin relaxation is determined by intra-valley scattering which does not depend on Λ_Γ.

C. Spin Lifetime and Valley Splitting

In Figure 7 we plot the variation of τ_S with the total valley splitting, c.f. Figure 5. One observes how τ_S strongly depends on the different possible values of Λ_Γ, particularly at the lower range of the valley splitting. The squared SR-induced intersubband spin relaxation matrix elements, normalized to the squared intrasubband scattering matrix elements at zero strain [20] ($M_{s,SR}$) and for a certain in-plane $\vec{k}$ vector, are shown in Figure 8. The sharp increase of $M^2_{s,SR}$ is located at the position where the valley splitting attains its minimum

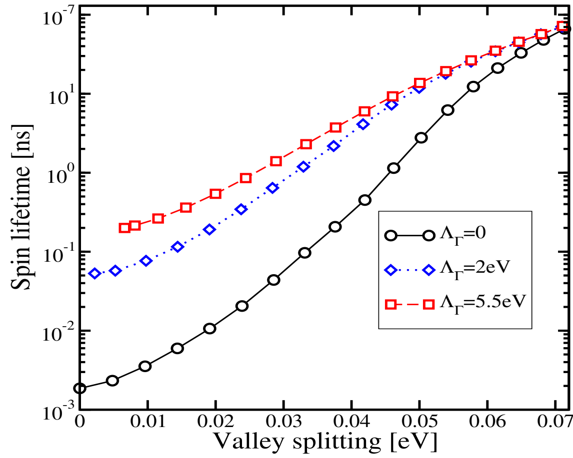

Fig. 7: Variation of the spin lifetime with the valley splitting results shown in Figure 5.

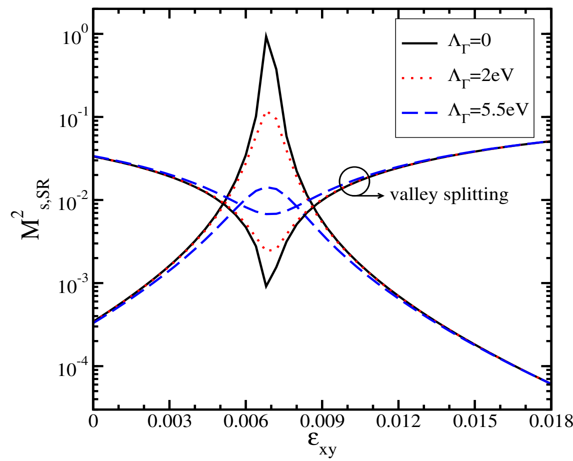

Fig. 8: Intersubband spin relaxation matrix elements as function of ε_{xy}, where k_x=0.3nm^{-1}, k_y=1nm^{-1}, and for different possible values for Λ_Γ. t=2.7nm.

value, and this occurs at the spin hot spot condition, which in turn is characterized by the large mixing of the up(down)-spin states [20] because

$$D\varepsilon_{xy} - \frac{\hbar^2 k_x k_y}{M} = 0\,. \quad (7)$$

Nevertheless, the behavior of the spin lifetime as delineated in Figure 7 is correlated with the suppression of the spin hot spot peaks with increasing $\triangle E_C$, as found in Figure 8. However, in all cases the spin lifetime is boosted by several orders of magnitude.

IV. Conclusion

We have discussed how shear strain-induced subband splitting causes a giant increase of spin lifetime in a thin silicon film. This enhancement is strongly sensitive to the different parameters like sample thickness, electron concentration, and operating temperature. We have explained that this is a consequence of the reduction of the intervalley spin relaxation. The possible values of the valley splitting in an unstrained structure are included, and their impact on the spin relaxation mechanisms is compared. It is concluded that in all cases the spin lifetime is boosted by at least two orders of magnitude. Therefore, shear strain routinely used to enhance mobility can also be used to boost spin lifetime.

Acknowledgment

This work is supported by the European Research Council through the grant #247056 MOSILSPIN. The computational results have been achieved in part using the Vienna Scientific Cluster (VSC).

References

[1] M. Bohr. The Evolution of Scaling from the Homogeneous Era to the Heterogeneous Era. In *Electron Devices Meeting (IEDM), 2011 IEEE International*, pages 1.1.1–1.1.6, 2011.

[2] D. E. Nikonov and I. A. Young. Overview of Beyond-CMOS Devices and a Uniform Methodology for their Benchmarking. *Proceedings of the IEEE*, 101(12):15, 2013.

[3] R. Jansen. Silicon Spintronics. *Nature Materials*, 11:400–408, 2012.

[4] B. Huang, D. J. Monsma, and I. Appelbaum. Coherent Spin Transport through a 350 Micron Thick Silicon Wafer. *Physical Review Letters*, 99:177209, 2007.

[5] S. P. Dash, S. Sharma, R. S. Patel, M. P. de Jong, and R. Jansen. Electrical Creation of Spin Polarization in Silicon at Room Temperature. *Nature*, 462:491–494, 2009.

[6] J. Li and I. Appelbaum. Modeling Spin Transport in Electrostatically-Gated Lateral-Channel Silicon Devices: Role of Interfacial Spin Relaxation. *Physical Review B*, 84:165318, 2011.

[7] D. Osintsev, V. Sverdlov, and S. Selberherr. Reduction of Momentum and Spin Relaxation Rate in Strained Thin Silicon Films. In *Proceedings of the Solid-State Device Research Conference (ESSDERC)*, pages 334–337, 2013.

[8] G.L. Bir and G.E. Pikus. *Symmetry and Strain-Induced Effects in Semiconductors*. J. Wiley and Sons, New York-Toronto, 1974.

[9] V. Sverdlov. Strain-Induced Effects in Advanced MOSFETs. Springer, Wien-New York, 2011.

[10] P. Li and H. Dery. Spin-orbit Symmetries of Conduction Electrons in Silicon. *Physical Review Letters*, 107:107203, 2011.

[11] T. Ando, A. B. Fowler, and F. Stern. Electronic Properties of Two-Dimensional Systems. *Reviews of Modern Physics*, 54:437–672, 1982.

[12] D. Osintsev, V. Sverdlov, N. Neophytou, and S. Selberherr. Valley Splitting and Spin Lifetime Enhancement in Strained Silicon Heterostructures. In *Proceedings of International Winterschool on New Developments in Solid State Physics*, pages 88–89, 2014.

[13] D. Rideau, M. Feraille, M. Michaillat, Y. M. Niquet, C. Tavernier, and H. Jaouen. On the Validity of the Effective Mass Approximation and the Luttinger $\mathbf{k}\cdot\mathbf{p}$ Model in Fully Depleted SOI MOSFETs. *Solid-State Electronics*, 53:452–461, 2009.

[14] T. B. Boykin, G. Klimeck, M. A. Eriksson, M. Friesen, S. N. Coppersmith, P. von Allmen, F. Oyafuso, and S. Lee. Valley Splitting in Strained Silicon Quantum wells. *Applied Physics Letters*, 84:115–117, 2004.

[15] Y. Song and H. Dery. Analysis of Phonon-induced Spin Relaxation Processes in Silicon. *Physical Review B*, 86:085201, 2012.

[16] M. V. Fischetti, Z. Ren, P. M. Solomon, M. Yang, and K. Rim. Six-band $\mathbf{k}\cdot\mathbf{p}$ Calculation of the Hole Mobility in Silicon Inversion Layers: Dependence on Surface Orientation, Strain, and Silicon Thickness. *Journal of Applied Physics*, 94(2):1079–1095, 2003.

[17] D. Esseni. On the Modeling of Surface Roughness Limited Mobility in SOI MOSFETs and its Correlation to the Transistor Effective Field. *IEEE Transactions on Electron Devices*, 51:394–401, 2004.

[18] C. Kittel. *Introduction to Solid State Physics*. Wiley, New York, 2004.

[19] J. Ghosh, D. Osintsev, V. Sverdlov, and S. Selberherr. Intersubband Spin Relaxation Reduction and Spin Lifetime Enhancement by Strain in SOI Structures. *Microelectronic Engineering*, 147(0):89–91, 2015.

[20] V. Sverdlov and S. Selberherr. Silicon Spintronics: Progress and Challenges. *Physics Reports*, 585:15–17, 2015.